Application of Small Angle Neutron Scattering to the *in Situ* Study of Protein Fouling on Ceramic Membranes

T. J. Su and J. R. Lu*

Department of Chemistry, University of Surrey, Guildford GU2 5XH, United Kingdom

Z. F. Cui

Department of Engineering, Parks Road, Oxford OX1 3PJ, United Kingdom

R. K. Thomas

Department of Physical and Theoretical Chemistry, South Parks Road, Oxford, OX1 3QZ, United Kingdom

R. K. Heenan

Rutherford Appleton Laboratory, Chilton, Didcot, OX11 0QX, United Kingdom

Received April 8, 1998. In Final Form: June 15, 1998

The fouling of ceramic ultrafiltration membranes by protein under dynamic filtration conditions has been investigated by small angle neutron scattering (SANS). Bovine serum albumin (BSA) solution was pumped through a thin commercial alumina membrane in a quartz cell specially designed to allow simultaneous SANS. SANS from clean membranes immersed in D_2O obeyed Porod's law and showed that the pores in these ultrafiltration membranes more closely resemble fractal or random pore structures than well-oriented, monodisperse arrays of cylindrical pores. During protein filtration, the SANS patterns showed a buildup with time of protein on all parts of this internal surface. The effects of time and pH indicate that the performance with respect to filtration is closely linked to the buildup of the adsorbed layer of protein.

Introduction

In the purification and separation of proteins by ultrafiltration, ceramic membranes offer the desirable properties of robustness, long service time, and ability to withstand harsh sterilization conditions. These properties make them potentially more useful than polymeric membranes, but their application in bioseparation and bioprocessing has been impaired by their poor biocompatibility. Fouling of the membrane by protein deposition in the membrane results in gradual blockage of the pores, and protein deposition often halts the filtration process in minutes.[1,2] Despite many investigations, the mechanism of fouling of the membrane is poorly understood. It has been suggested that fouling occurs as a result of adsorption of protein on the internal surface of the pores, by formation of a gel layer on the high-pressure side of the membrane by concentration polarization, or by some combination of both processes.[1−5] The early stages of development of the foulant layers are thought to be crucial to the understanding of fouling. However, the evolution of the structure of the protein foulant layer under operational conditions has not been studied because of a lack of experimental techniques for exploring the structure of wet interfaces. Measurements of the change in pore size, the total amount of adsorbed protein, together with contact angle and electron paramagnetic resonance studies,[1,6] all indicate that substantial adsorption of protein onto the surface of the membrane occurs in the first few minutes. Most of these methods require removal of the membrane from the filtration system. For a better assessment of the existence of an adsorbed layer and its role in the fouling process it is highly desirable to develop an *in situ* technique to monitor the buildup of the foulant layer.

Small angle neutron scattering (SANS) is an established technique for investigating the structure and distribution of small particles and is particularly effective for the study of aqueous dispersions.[7] Although the majority of SANS measurements have been on aggregates in solution, SANS has been shown to be equally effective in the study of porous systems, especially where water is involved. Because ceramic membrane materials such as silica and alumina are reasonably transparent to neutrons, it should be possible to use SANS to monitor the gradual deposition of protein within membrane pores by following the changes in scattering intensity with time. In this paper, we present the first such study, using alumina membranes prepared by anodization[8] and bovine serum albumin (BSA), which is a well-characterized protein.[9−11]

(1) Marshall, A. D.; Munro, P. A.; Tragardh, G. *Desalination* **1993**, *91*, 65.
(2) Bowen, W. R.; Hughes, D. T. *J. Membr. Sci.* **1990**, *51*, 189.
(3) Le, M. S.; Howell, J. A. In *Progress in Food Engineering*; Cantarelli, C.; Peri, C., Eds.; Forster-Verlag: Kusnacht, 1983; p 321.
(4) Larsson, K. *Desalination* **1980**, *35*, 105.
(5) Gekas, V. *Desalination* **1988**, *68*, 77.
(6) Oppenheim, S. F.; Phillips, C. B.; Rodgers, V. G. J. *J. Colloid Interface Sci.* **1996**, *184*, 639.
(7) Hodge, D. J., Laughlin, R. G.; Ottewill, R. H.; Rennie, A. R. *Langmuir* **1991**, *7*, 878.
(8) Furneaux, R. C.; Rigby, W. R.; Davidson, A. P. *Nature* **1989**, *337*, 147.
(9) Fane, A. G.; Fell, C. J. D.; McDonogh, R. M.; Suki, A.; Waters, A. G. In *Proceedings 11th Australian Conferences Chemical Engineering (Chemeca 83)*, Brisbane, 1983; p 729.

S0743-7463(98)00392-8 CCC: $15.00
Published on Web 08/26/1998

We selected alumina membranes for the experiment because the pores produced by anodization are thought to be reasonably separated with only a low interconnecting fraction.[8] For a perfectly cylindrical pore aligned along the direction of the beam, the scattering pattern consists of a series of radial fringes (Airy fringes) whose spacing is inversely related to the diameter of the pore and whose intensity depends on the contrast between the alumina forming the pore wall and the contents of the pore. This contrast is determined by the difference in scattering length density between alumina and that of the pore contents. The scattering length density is given by

$$\rho = \sum_i n_i b_i \qquad (1)$$

where b_i and n_i are the scattering length and number density, respectively, of the constituent atoms. The difference in the scattering length density between alumina and air is such that a good signal can be obtained from the dry membrane and from the membrane fully impregnated with either H_2O or D_2O. More importantly, because H and D nuclei scatter neutrons with different phases and amplitudes, it is possible to adjust the contrast between alumina and water by varying the isotopic composition of the water. In particular, the composition of the water can be adjusted so that a composite pore wall consisting of alumina and protein can be made visible. Thus, in D_2O, the Airy fringes produced by an ideal cylindrical pore would be substantially modified by the presence of adsorbed protein.

Experimental Section

The key to the experiment was to construct a flow cell that could function both as a normal filtration unit and a suitable cell for the neutron scattering measurement (Figure 1). The scattering geometry requires the collimated neutron beam to be perpendicular to the ceramic membrane. Within the quartz windowed cell, patterned frames were used to support the membrane to prevent it from deforming under the pressure applied during flow and to distribute the flow to make the flux more uniform across the face of the membrane. The filtration was operated in a cross-flow mode, similar to that normally used in practical operations. The membrane cell was initially primed with aqueous solution, and the solution was circulated by a peristaltic pump at the typically operational pressure of 0.5 bar.

The SANS measurements were made on the white beam time-of-flight scattering instrument LOQ at the Rutherford-Appleton Laboratory, ISIS, Didcot, UK, which has a wavelength range 2−10 Å.[12] The procedure for performing the measurements was similar to that described previously for the study of surfactant aggregation.[7] The sample cell was mounted on the translational table and its position was aligned using a laser beam that shared the same beam path as the neutron beam. The absolute scattering intensity of the instrument was calibrated with respect to a partially deuterated polystyrene standard with known scattering intensity. The background was determined by measuring the scattering from the sample cell without the membrane in place. All the experiments were performed in buffered D_2O at 298 K.

Alumina membranes were purchased from Whatman (Anodisc 25) and had a nominal pore diameter of 200 Å. Fatty acid-free BSA was purchased from Sigma (99%) and was used as supplied. D_2O (99.9% D) was supplied by Fluorochem, and its purity was assessed by surface tension measurement. The purity was typically >71 mN m^{-1} at 298 K, indicating the absence of any surface active impurity. H_2O was processed through an Elgastat

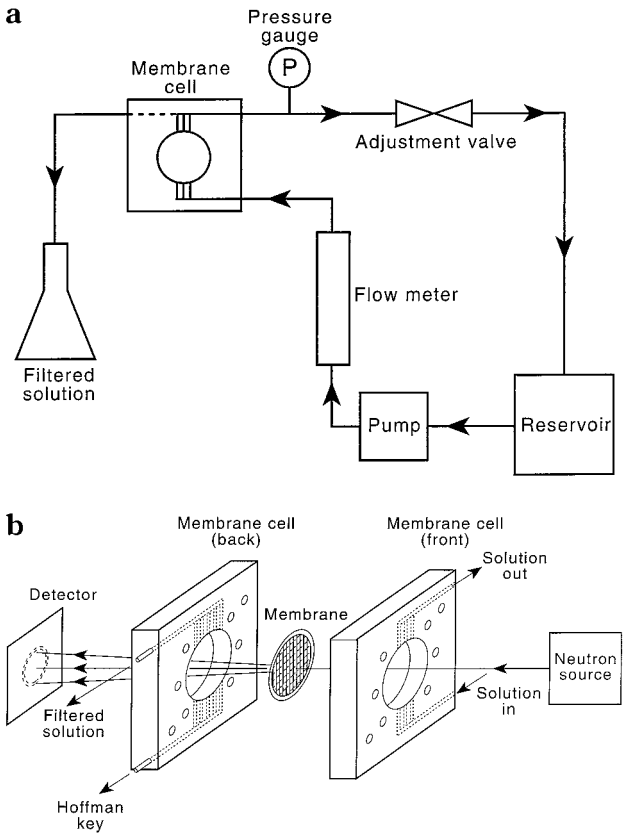

Figure 1. Schematic diagram of (a) the filtration system and (b) the filtration cell in the neutron small-angle scattering beam. Under operational and scattering conditions, the alumina membrane is fully immersed in D_2O solution.

ultrapure water system (UHQ), and its surface tension at 298 K was constant at 71.5 mN m^{-1}. The solution pH was controlled by using phosphate buffer [Na_2HPO_4/NaH_2PO_4 at pH 7(± 0.2) and H_3PO_4/NaH_2PO_4 at pH 5], and the total ionic strength was fixed at 0.02 M. The glassware and the filtration system were cleaned with alkaline detergent (Decon 90) followed by repeated washing in UHQ water.

Results and Discussion

The SANS measurements were first performed on the bare membranes in buffered D_2O to characterize the scattering patterns of the membranes themselves. Literature results have shown that scattering from silica powders and porous alumina samples with random pore structure follows Porod's law, in which the scattering intensity is proportional to κ^{-4}.[13−15] Figure 2 shows the plot of the absolute scattering intensity in terms of log $I(\kappa)$ as a function of log κ for the bare membrane immersed in D_2O, where κ is the momentum transfer ($\kappa = 4\pi \sin\theta/2$, where 2θ is the scattering angle and λ is the beam wavelength). The linear relationship between log $I(\kappa)$ and log κ with the exact Porod slope of -4 ± 0.3 over most of the accessible range of κ confirms that the scattering from the membrane follows Porod's law. The error quoted for the slope of the graph in Figure 2 includes the range of variation in the slope over the higher range of κ and the uncertainties in the determination of the background. Below a κ value of about 0.02 $Å^{-1}$, the slope is steeper.

(10) Turker, M.; Hubble, J. *J. Membr. Sci.* **1987**, *34*, 267.
(11) Bowen, W. R.; Calvo, J. I.; Hernandez, A. *J. Membr. Sci.* **1995**, *101*, 153.
(12) Heenan, R. K.; Penfold, J.; King, S. M. *J. Appl. Crystallogr.* **1997**, *30*, 1140.
(13) Schmidt, P. W. *J. Appl. Crystallogr.* **1991**, *24*, 414.
(14) Schmidt, P. W.; Avnir, D.; Levy, D.; Höhr, A.; Steiner, M.; Röll, A. *J. Am. Phys.* **1991**, *94*, 1474.
(15) Mitropoulos, A. C.; Steriotis, T. A.; Katsaros, F. K.; Tzevelekos, K. P.; Kanellopoulos, N. K.; Keiderling, U.; Sturm, A.; Wiedenmann, A. *J. Membr. Sci.* **1997**, *129*, 289.

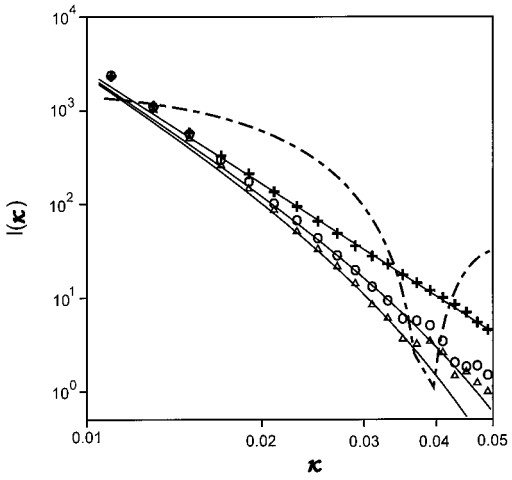

Figure 2. Variation of $I(\kappa)$ with κ for the fouling of the membrane in 0.1 g dm^{-3} BSA solution in buffered D_2O at pH 5 at times of 10 (o) and 120 min (Δ). The scattering intensity from the bare membrane in D_2O is also shown for comparison (+). The continuous lines were fitted by eq 2 with a slope of 4 ± 0.3 for the bare membrane and by eq 3 with $\sigma = 27 \pm 3$ Å for the measurement at 10 min and $\sigma = 35 \pm 3$ Å for the measurement at 120 min. The values of $I(\kappa)$ are in units of cm^{-1} and κ is in Å^{-1}. The scattering from an array of perfect cylindrical pores of the nominal diameter of 200 Å is shown as a dashed line. The pore density was taken to be 1.1×10^9 cm^{-2} from ref 8. Uncertainty in pore density only affects the level of the curve, but not the shape.

However, Porod's law only holds at the limit of high κ (κd must be much greater than unity, where d is the diameter of the pore), and this deviation probably results from the detailed structure of the membrane pores. Porod's law holds only when the interface between the two materials forming the pore is perfectly sharp; it does not apply when there is a gradual step in scattering length density across the interface. The results therefore suggest that the scattering in the high κ region results from the internal surface of the pores and that this surface is a sharp step between alumina and the D_2O filling the pores.

Calculation of the SANS intensity for an array of perfect end-on cylindrical pores is relatively straightforward,[16] and this is very different in shape from the observed (see dashed line in Figure 2). Indeed, the scattering is much better explained by assuming a random pore structure. This result is not surprising because although, in principle, the pores have been generated as parallel cylinders by the anodizing process, the shape and size of the actual pores are highly irregular, as observed by scanning electron microscopy (SEM).[8] We have performed SEM measurements on our own batch of anodized alumina membranes (Figure 3) and found an even greater variation in pore shape and size distribution than observed for the membranes examined in ref 8. The surface area of the pores can be estimated from the exact expression for Porod's law[17]

$$I(\kappa) = 2\pi A(\Delta\rho)^2 \kappa^{-4} \qquad (2)$$

where $\Delta\rho$ is the contrast difference between the water and alumina (1.75×10^{-6} Å^{-2}) and A is the area of the internal pore surface per unit volume. From the slope of the plots in Figure 2, A was found to be 0.014 Å^{-1} for a membrane with nominal pore diameter of 200 Å. The

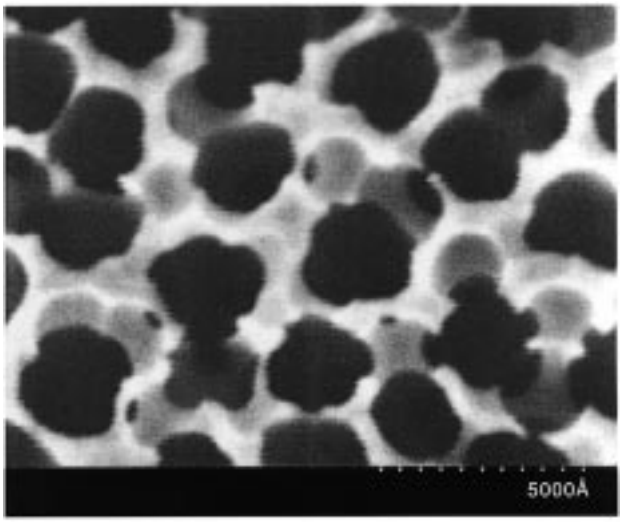

Figure 3. Scanning electron micrograph of the membrane with nominal pore diameter 200 Å. The smaller pores are the gray spots in the background and are out of focus.

total internal surface area obtained from SANS is almost twice the value derived from application of a simple hydrodynamic relation to the diffusivity through the pores based on the assumption that the pores are cylindrical and monodisperse.[1,2,11] This result further suggests that the actual pores are less regular than the simple model.

The development of the fouling of the membranes was followed by the variation of SANS intensity with time. The gradual buildup of BSA at pH 5 and at a bulk BSA concentration of 0.1 g dm^{-3} in the membrane is shown in Figure 2. The SANS measurements were made twice: 10 min after the start of filtration when the flux through the membrane was ~60% of the initial rate and 120 min from the start when the filtration had almost completely stopped. To minimize any contribution of protein molecules in the bulk solution to the scattering, the external solution in the cell was displaced by pure buffered D_2O immediately before each scattering measurement. This replacement of solution had no observable effect on the flux through the membrane, showing that it did not disturb the fouling protein layer. In comparison with the scattering from the clean membrane, the accumulation of protein in the membrane resulted in a steeper decay in the plot of log $I(\kappa)$ versus log κ. Also, the longer the filtration process had been running, the steeper was the slope. This increased slope in the scattering plots is the same as observed for silica particles when coated with alkyl chains. Schmidt et al.[13,14] have studied the effect of alkyl chain length on the small angle X-ray scattering from porous silica, onto which chains have been grafted, and found that the slope of the Porod plot increases with the chain length of the grafted alkyl chain and with coverage. Using SANS, Glinka et al.[18] found a similar trend with respect to the effects of chain length and surface coverage, although they used a different method of analyzing the data. Comparison of these results, which are from closely related systems, suggests that the increased decay in the plots of log $I(\kappa)$ versus log κ is caused by adsorption of protein onto the internal surface of the pores and that the amount adsorbed increases with time.

In treating porous dispersions with diffuse interfaces, Ruland and others[19−21] have approximated the local

(16) Oster, G.; Riley, D. P. *Acta Crystallogr.* **1952**, *5*, 272.
(17) Porod, G. In *Small Angle X-ray Scattering*; Glatter, O.; Kratky, O., Eds.; Academic: New York, 1982.
(18) Glinka, C. J.; Sander, L. C.; Wise, S. A.; Berk, N. F. *Mat. Res. Soc. Symp. Proc.* **1990**, *166*, 415.
(19) Ruland, W. *J. Appl. Crystallogr.* **1971**, *7*, 383.

variation of the scattering length density to a step profile convoluted with a smoothing function. If a Gaussian smoothing function is chosen, the effect of the presence of diffuse interface on the scattering intensity can be written as

$$I(\kappa) = \frac{2\pi A(\Delta\rho)^2}{\kappa^4} \exp(-\kappa^2\sigma^2) \qquad (3)$$

where σ is the width of the diffuse interface and is therefore an approximate measure of the thickness of the adsorbed layer on the surface of the pores. When $\sigma \rightarrow 0$, eq 3 becomes Porod's law and the introduction of the exponential term leads to a decay steeper than κ^{-4}. The continuous lines through the data in Figure 2 were fitted using eq 3 to give values of σ of 27 ± 3 and 35 ± 3 Å after 10 and 120 min, respectively. The results therefore suggest that a substantial amount of protein is adsorbed on to the surface of the pores after just 10 min of filtration and that by the time the permeating flux has almost declined to zero, the thickness of the adsorbed layer of protein has further increased. A similar trend was also observed by Bowen et al.[2] using an assay to determine the BSA adsorption. Our results confirm the validity of Bowen's method but give the additional information that the protein is uniformly distributed over the whole of the available internal surface of the membrane. Although our model only gives an approximate estimate of the relative thickness of the layer, there is no ambiguity about the progressive increase in the amount of adsorbed protein. That eq 3 fits the measured scattering intensities well again suggests that the scattering behavior of this type of membrane resembles that of randomly structured porous membranes, particulate dispersions, microemulsions, and polymer suspensions with diffuse interfaces.[19−21] This result is partly because the technique probes the smaller scale structure in the membrane rather than the large scale geometry.

The effect of pH on the structure of the foulant layers was also studied. Scattering measurements were made at pH 5 and 7, at a bulk lysozyme concentration of 1 g dm^{-3}, and, in each case, after the filtration had been run for 120 min. The results are shown in Figure 4. After 120 min, the permeating flux was almost zero at pH 5 and ~15% of the initial rate at pH 7. Because the isoelectric point for BSA is at pH 4.8, the amount of adsorbed protein is expected to peak at this pH. At pH 7, the amount of protein adsorbed should be reduced because the net charge on BSA has the same sign as that of the alumina surface, leading to an increase in the effects of repulsion on the layer. The observed scattering intensities plotted in Figure 4 do indeed show a large difference between the two pH values, which indicates a large difference in the extent of fouling. These differences are qualitatively consistent with the observed effects on the filtration process.[2,11] The values of the thickness parameter σ were 15 ± 3 Å at pH 7 and 43 ± 3 Å at pH 5, suggesting that the fouled layer at pH 5 is much thicker than at pH 7.

Although the model presented is only approximate, it does demonstrate the link between adsorption of protein and fouling and through this link, it offers a simple means of estimating the variation of fouling with system conditions. The major assumption in applying eq 3 is that there is a monotonic decay in the scattering length density between D_2O and alumina.[19−21] The scattering length density of the alumina is 4.6×10^{-6} $Å^{-2}$, that of D_2O is 6.35×10^{-6} $Å^{-2}$, and that of BSA (in D_2O) is 3.2×10^{-6} $Å^{-2}$. Our own recent neutron reflection study of BSA adsorption onto a flat hydrophilic silicon oxide surface shows that the maximum volume fraction of BSA in the layer is always <0.55.[22] If this also holds for the adsorption on alumina, the scattering length density of the mixed BSA/water layer will always lie between those of alumina and D_2O and the assumption of a monotonic decay in the scattering length density is then a reasonable one. In the calculation of the scattering length density of the BSA we have assumed that there is complete exchange of the labile hydrogens in the protein. We have shown elsewhere that >80% of the labile hydrogens exchange within 2 h and any further uncertainty in the exchange rate will not affect our basic assumption.[22]

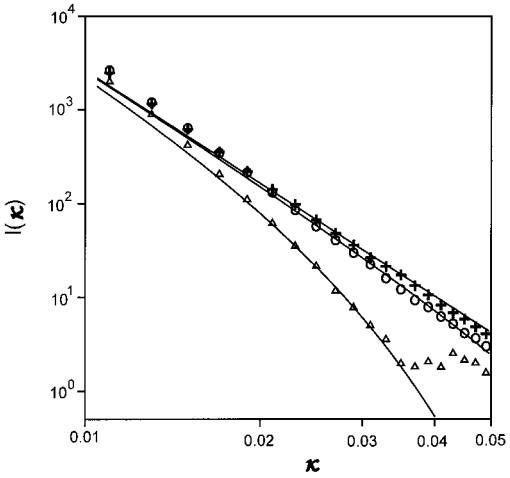

Figure 4. Variation of $I(\kappa)$ with κ for the fouling of the membrane in 1 g dm^{-3} BSA solution in buffered D_2O at pH 7 (o) and pH 5 (Δ). The scattering intensity from the bare membrane in D_2O is also shown for comparison (+). The continuous lines were fitted using eq 2 with a slope of 4 ± 0.3 for the bare membrane and using eq 3 with σ = 15 ± 3 Å for the measurement at pH 7 and σ = 43 ± 3 Å at pH 5. Both measurements were made after the filtration had run for 120 min. The values of $I(\kappa)$ are in units of cm^{-1} and κ is in $Å^{-1}$.

The main result of this work therefore demonstrates that SANS is a sensitive technique for monitoring the *in situ* development of the foulant layer inside the membrane pores. Although a simple model has been used for the data analysis, the straightforward handling of the results clearly shows how scattering intensity varies with the gradual buildup of adsorbed protein on the surface of the membrane pores. The values obtained for the surface area indicate that SANS measures the whole internal surface area of the pores rather than just those small pores within the thin skin on the front surface of the membrane. The change in scattering pattern following filtration of protein demonstrates the sensitivity of the scattering to the protein layer deposited on this internal surface and shows that it is the whole pore surface that is covered with protein. We expect in subsequent work to develop more precise mathematical models relating the structure of this adsorbed layer to the scattering and to utilize more extensively the possibility of varying the contrast of scattering length density between water and alumina.

LA980392B

(20) Hashimoto, T.; Todo, A.; Itoi, H.; Kawai, H. *Macromolecules* **1977**, *10*, 377.
(21) Strey, R.; Winker, J.; Magid, L. *J. Phys. Chem.* **1991**, *95*, 7502.
(22) Su, T. J.; Lu, J. R.; Thomas, R. K.; Cui, Z. F.; Penfold, J. *J. Phys. Chem. B.*, in press.